



Article

Effector Sntf2 Interacted with Chloroplast-Related Protein Mdyfc39 Promoting the Colonization of *Colletotrichum gloeosporioides* in Apple Leaf

Meiyu Wang , Zhirui Ji , Haifeng Yan, Jie Xu, Xuanzhu Zhao and Zongshan Zhou *

Research Institute of Pomology, Chinese Academy of Agricultural Sciences, Xingcheng 125100, China; wang903108175@163.com (M.W.); xinyu_jzr@163.com (Z.J.); yanhaifeng50@163.com (H.Y.); szpyzt@163.com (J.X.); 72109019@mail.edu.cn (X.Z.)

* Correspondence: zszhouqrj@163.com

Abstract: Glomerella leaf spot of apple, caused by *Colletotrichum gloeosporioides*, is a devastating disease that leads to severe defoliation and fruit spots. The *Colletotrichum* species secretes a series of effectors to manipulate the host's immune response, facilitating its colonization in plants. However, the mechanism by which the effector of *C. gloeosporioides* inhibits the defenses of the host remains unclear. In this study, we reported a novel effector Sntf2 of *C. gloeosporioides*. The transient expression of *SNTF2* inhibits BAX-induced cell death in tobacco plants. Sntf2 suppresses plant defense responses by reducing callose deposition and H₂O₂ accumulation. *SNTF2* is upregulated during infection, and its deletion reduces virulence to the plant. Sntf2 is localized to the chloroplasts and interacts with Mdyfc39 (a chloroplast PSII assembly factor) in apple leaves. The *Mdyfc39* overexpression line increases susceptibility to *C. gloeosporioides*, whereas the *Mdyfc39* transgenic silent line does not grow normally with pale white leaves, indicating that Sntf2 disturbs plant defense responses and growth by targeting Mdyfc39.



Citation: Wang, M.; Ji, Z.; Yan, H.; Xu, J.; Zhao, X.; Zhou, Z. Effector Sntf2 Interacted with Chloroplast-Related Protein Mdyfc39 Promoting the Colonization of *Colletotrichum gloeosporioides* in Apple Leaf. *Int. J. Mol. Sci.* **2022**, *23*, 6379. <https://doi.org/10.3390/ijms23126379>

Academic Editor: Fucheng Lin

Received: 18 April 2022

Accepted: 4 June 2022

Published: 7 June 2022

Publisher's Note: MDPI stays neutral with regard to jurisdictional claims in published maps and institutional affiliations.



Copyright: © 2022 by the authors. Licensee MDPI, Basel, Switzerland. This article is an open access article distributed under the terms and conditions of the Creative Commons Attribution (CC BY) license (<https://creativecommons.org/licenses/by/4.0/>).

Keywords: *Colletotrichum*; effector; pathogenicity; immune response; apple

1. Introduction

In agricultural and natural ecosystems, plants are exposed to numerous pathogens. Nevertheless, plants have complex defense systems to combat pathogen invasion [1]. When pathogen-associated molecular patterns (PAMPs) are recognized by pattern recognition receptors (PRRs) on the cell surface, the plant's basal defense response is activated, termed PAMP-triggered immunity (PTI) [2]. Damage-associated molecular patterns (DAMPs)-triggered immunity (DTI) plays an important role in a plant's basal defense response [3,4]. Plants have evolved intracellular nucleotide-binding leucine-rich-repeat receptors (NLRs) to recognize pathogen effectors directly or indirectly, leading to activation of the second line of defense, known as effector-triggered immunity (ETI) [2]. However, pathogens secrete a series of virulence effectors that interfere with the plant's immune system, promoting pathogen invasion [5,6]. Hence, exploring the virulence mechanisms of effectors is important for revealing the infection strategies of plant pathogens.

The *Colletotrichum* species, belonging to Glomerellaceae of Ascomycota, develop penetration pegs from appressoria to invade the host [7]. *Colletotrichum* deploys distinct effectors at different infection phases to manipulate the host plant's immune response [8]. Although various effectors have been identified [9,10], few have investigated their specific function mechanisms [11,12]. The interaction mechanism between effectors and host target proteins of *Colletotrichum* mainly focused on *Colletotrichum higginsianum*, *Colletotrichum fruticola*, and *Colletotrichum orbiculare* [13–15]. Each *Colletotrichum* species has evolved a set of effectors with unique strategies to adapt to its host plants [16]. In *C. gloeosporioides*, many studies focused on identifying the pathogenicity-related genes [17,18], but few focused on

characterizing the mechanisms of effectors in the interactions between *C. gloeosporioides* and host plants.

C. gloeosporioides is a plant pathogenic fungus that infects various plants, including apple, mango, and poplar [19]. Glomerella leaf spot of apple (GLSA), caused by *C. gloeosporioides*, is a devastating disease that severely affects apple production [20,21]. Under favorable conditions, the latent period of this disease is as short as two days, and it spreads rapidly [19,22], causing necrotic fruit spots and severe defoliation in 'Royal Gala' and 'Golden Delicious' apples. To date, the control of GLSA remains a challenge. Understanding the molecular interactions between *C. gloeosporioides* and apples is instrumental for sustaining effective disease control and developing disease-resistant varieties.

Chloroplasts not only play a role as photosynthetic organelles but also play a central role in plant defense by integrating environmental stimuli and the determinants of downstream defense responses [23–25]. Upon perception of pathogenic threat, chloroplast as the source of calcium, salicylic acid (SA), and reactive oxygen species (ROS) bursts communicates with the nucleus through retrograde signaling [24], mediates activation of plant immune signaling, and leads to the expression of defense-related genes [26,27]. To interfere with the function of chloroplasts in the interaction between the pathogens and the hosts, pathogens, including bacteria, viruses, fungi, and Oomycetes, have deployed effectors to target chloroplasts [6,23,27–29]. However, the underlying mechanisms with which effectors target chloroplasts to manipulate the host's defenses have remained elusive in *Colletotrichum*.

In this study, we found that a novel effector Sntf2 of *C. gloeosporioides* played an essential role in suppressing the plant's defense responses. Sntf2 is an extracellular-secreted protein including a signal peptide in its N-terminal, which plays a vital role in plant infection. Consistent with this, the deletion of *SNTF2* triggered the plant's defense responses, in which H₂O₂ accumulation and callose deposition increased in the apple leaves inoculated with the Δ sntf2-1 mutant. We showed that Sntf2 could inhibit Bcl-2-associated X protein (BAX)-induced cell death, suppressing hypersensitive responses in plants. Our investigation demonstrated that Sntf2 could migrate into a host plant's cells and interact with the Mdyfc39 (a photosystem II assembly factor of *Malus domestica*). We also found that Mdyfc39 played a vital role in plant resistance and development. Overall, our results show that Sntf2 perturbs the function of chloroplast, avoiding to trigger cell death and supporting pathogen colonization on live plants.

2. Results

2.1. Sntf2 Inhibits BAX-Induced Cell Death in Tobacco

BAX, a pro-apoptotic protein, stimulates cell death, which closely resembles the hypersensitive responsive (HR) in plants [30]. *SNTF2* (CGGC5_13909) encodes a putative protein in *C. gloeosporioides* with 187 amino acid residues and contains a predicted signal peptide (SP; 1–20 aa) (Figure 1a). To investigate if Sntf2 inhibited a plant's innate immunity, we performed transient expression of the gene in *Nicotiana benthamiana*. The *Agrobacterium* strain GV3101 carrying the potato virus X (PVX) vector pGR106-fused *SNTF2* gene was infiltrated into the leaves of *N. benthamiana*, and the strain carrying pGR106-BAX was injected into the same sites on the leaves after 24 h post-infiltration. We found that Sntf2 suppressed the cell death triggered by BAX in the infiltrated leaves (Figure 1b). These data indicated that Sntf2 suppressed the HR response of the plant.

2.2. SNTF2 Is Upregulated during Biotrophic Infection Phase

To analyze the expression pattern of *SNTF2* at different infection phases, the transcripts of *SNTF2* were examined in infected leaves at 12, 24, 48, and 72 h post-inoculation (hpi) using qRT-PCR. *SNTF2* was upregulated at 24 hpi and 48 hpi (Figure 2). Appressoria formed at 12 hpi, and appressorium-mediated penetration occurred at 24 hpi (Figure S1). Fungal primary infection hyphae formed at 48 hpi (Figure S1). This meant that *SNTF2* was highly expressed from appressorium-mediated penetration to infection-hyphae formation.

In addition, fluorescence signal detection showed that *Sntf2*-eGFP was actually expressed during the infection in apple leaves (Figure S1). These results suggest that *SNTF2* may play an important role in plant infection.

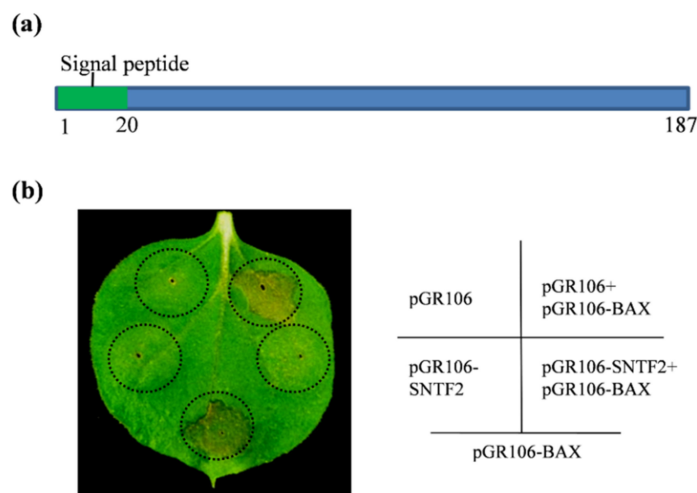


Figure 1. *Sntf2* suppressed BAX-triggered cell death in *Nicotiana benthamiana*. (a) The structure analysis of *Sntf2*. *Sntf2* was predicted to contain an N-terminal signal peptide (1–20 aa). (b) The tobacco leaves infiltrated with *Agrobacterium tumefaciens* GV3101 harboring the pGR106 vector or the vector with *SNTF2* inserted. The *A. tumefaciens* carrying the *BAX* gene were injected into the leaves after 24 h post-infiltration. The empty pGR106 vector was used as the control. The black dotted lines indicate the region of infiltration. The diagram on the right shows the transformant strains of *A. tumefaciens* (containing recombinant pGR106 vectors) that was injected inside the black dotted lines. Images were acquired at 7 days post-infiltration. The experiments were repeated six times.

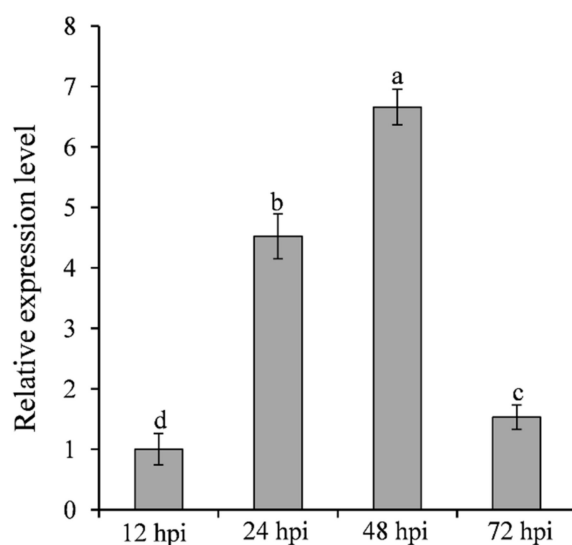


Figure 2. Analysis of *SNTF2* transcription at different infection phases by qRT-PCR. The cDNA was obtained from the apple leaves at 12, 24, 48, and 72 h post-inoculation (hpi) with *Colletotrichum gloeosporioides*. The *M. domestica* ubiquitin extension factor (*MdUBQ*) gene was used as the reference gene to normalize and analysis the transcription of *SNTF2*. Results were presented as the average fold values from three independent experiments compared with 12 hpi samples. Error bars represent standard deviations. Lowercase letters indicate significant differences ($p < 0.01$).

2.3. *Sntf2* Is Required for the Pathogenicity of *C. gloeosporioides*

To determine the function of *SNTF2* in the pathogenicity, *SNTF2* deletion mutants were constructed using *A. tumefaciens*-mediated homologous recombination (Figure S2a).

The $\Delta sntf2$ mutants were confirmed by PCR and Southern blot analysis (Figure S2b–d). The complementation strain $\Delta sntf2-1/SNTF2$ was generated and validated by PCR analysis (Figure S2c,d). The $\Delta sntf2$ mutant had a normal growth rate compared with the wild type, as well as conidial production, appressorial formation, and invasive pegs formation (Figure S3). The apple leaves inoculated with the $\Delta sntf2$ mutants showed tiny spots compared with the WT (Figure 3), indicating that *Sntf2* was required for the pathogenicity of *C. gloeosporioides*.

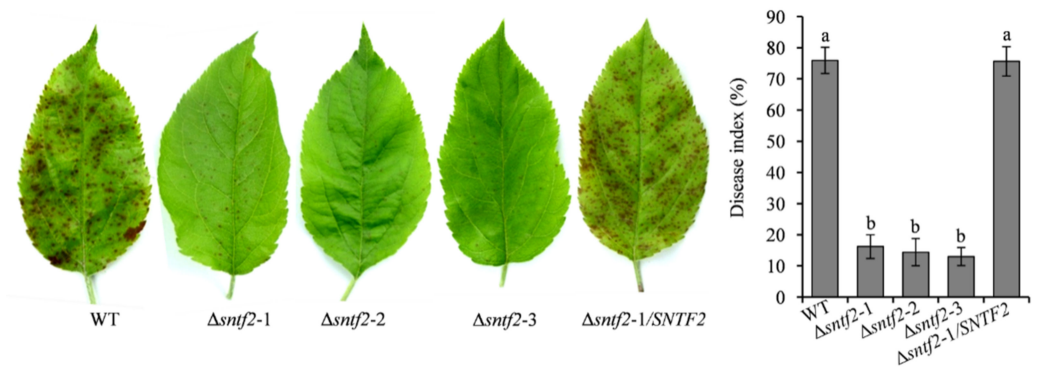


Figure 3. *SNTF2* deletion reduced the pathogenicity of *Colletotrichum gloeosporioides*. The pathogenicity was evaluated based on the disease index. Each experiment was repeated three times with ten leaves used for each replicate. Error bars represent standard deviations. Lowercase letters indicate significant differences ($p < 0.01$).

2.4. *Sntf2* Suppresses Apple Defense Responses

To evaluate if *Sntf2* suppressed apple defense responses during the infection, we tested the generation of H_2O_2 and callose in apple leaves. The 3,3'-diaminobenzidine (DAB) staining result showed that H_2O_2 accumulation increased at the invasive sites when inoculated with the $\Delta sntf2-1$ mutant compared with the WT (Figure S4a). The H_2O_2 accumulation in the apple leaves inoculated with the complementation strain $\Delta sntf2-1/SNTF2$ was similar to the WT (Figure 4a). The rate of callose formation in apple leaves inoculated with the $\Delta sntf2-1$ mutant was 24.4% higher than the leaves inoculated with the WT (Figure 4b). Aniline blue staining also showed that callose deposition in leaves inoculated with the $\Delta sntf2-1$ mutant increased at 36 hpi compared with the WT (Figure S4b). These results indicated that the deletion of *SNTF2* triggered apple defense responses.

2.5. *Sntf2* Is a Secretion Protein

SignalP 4.0 analysis revealed that a SP was present in *Sntf2* (SP; 1–20 aa; Figure 1a). To verify the function of this SP, an expression vector harboring the yeast invertase sequence fused to the SP was constructed and transformed into yeast strain YTK12. The transformant containing pSUC2-SP_{SNTF2} could grow on YPRAA plates (Figure 5a), which was consistent with the positive Avr1b [31], indicating that the SP of *Sntf2* was able to secrete invertase. The invertase secreted by the transformant was confirmed by using 2, 3, 5-triphenyltetrazolium chloride (TTC) assays (Figure S5b). To observe the extracellular secretion of *Sntf2*, we constructed a *Sntf2*-eGFP expression strain. We found that *Sntf2*-eGFP was secreted into plant cells (Figure 5b and Figure S1). These results revealed that the SP of *Sntf2* was functional in mediating the extracellular secretion of *Sntf2*. Expectedly, the complementation mutant $\Delta sntf2-1/SNTF2^{\Delta SP}$ did not restore fully the pathogenicity of the $\Delta sntf2-1$ strain (Figure S5c,d), indicating that the SP of *Sntf2* played a vital role in plant infection.

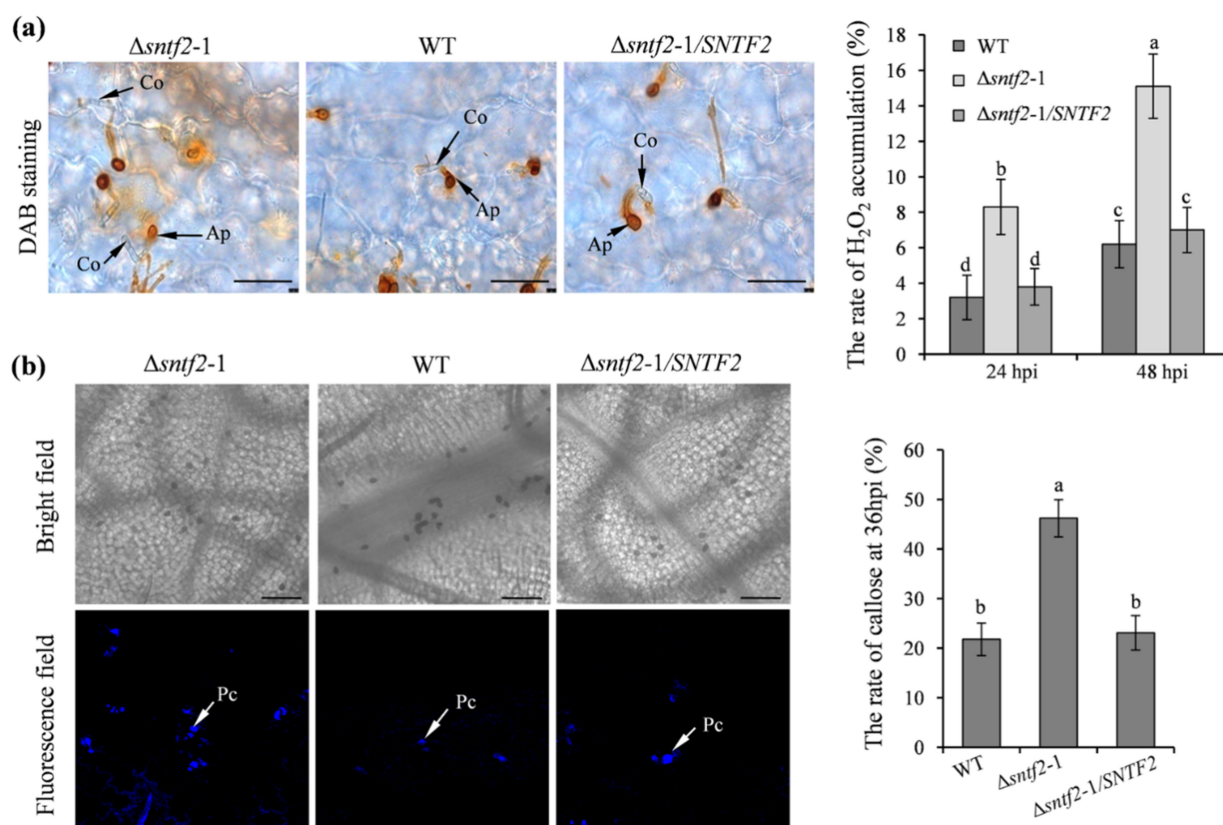


Figure 4. The H_2O_2 accumulation and callose deposition in apple leaves during the infection. (a) DAB staining was performed to detect H_2O_2 accumulation on apple leaves. DAB oxidation led to brownish polymer formation that was deposited at the site of H_2O_2 accumulation. Co: conidia; Ap: appressorium; bar: 50 μ m. (b) Aniline blue staining was to observe callose deposition on apple leaves at 36 hpi. Apple leaves were inoculated with WT, $\Delta sntf2-1$, $\Delta sntf2-2$, $\Delta sntf2-3$, or $\Delta sntf2-1/SNTF2$ strains. Pc: callose deposition; bar: 50 μ m. The rate of H_2O_2 accumulation and callose formation was evaluated. Error bars represent standard deviations. Lowercase letters represent significant differences ($p < 0.01$).

2.6. *Sntf2* Is Localized to Plant Chloroplasts

To observe the subcellular localization of *Sntf2*, we transiently expressed the *Sntf2*^{ΔSP}-eGFP fusion protein using *A. tumefaciens* LBA4404 infiltration in *N. benthamiana*. We found that the fluorescence signal of *Sntf2*^{ΔSP}-eGFP fusion proteins overlapped with the chloroplast autofluorescence signal (Figure 6). The localization analysis showed that the *Sntf2*^{ΔSP}-eGFP was mainly presented in chloroplasts.

2.7. *Sntf2* Interacts with the Photosystem II Assembly Factor *Mdyfc39*

To investigate *Sntf2*-interacting proteins, we performed a yeast two-hybrid (Y2H) screening assay. Twelve distinct putative interactors were confirmed via re-transformation into yeast (Table S1 and Figure S6). One of twelve positive genes encoded a chloroplast photosystem II assembly factor (MD05G1131800) (Table S1). We designated the gene as *Mdyfc39* since it was annotated as an *ycf39*-like protein in *Malus domestica* (NCBI databases). *Mdyfc39* is highly conserved with other *ycf39*-like proteins identified from plant species including *Arabidopsis thaliana* [32] (80.76% identity to HCF244; Figure S7a). The *Mdyfc39* contained a predicted chloroplast-targeting sequence (cTP; 27–64 aa) and a NAD(P)-binding domain (Figure 7a).

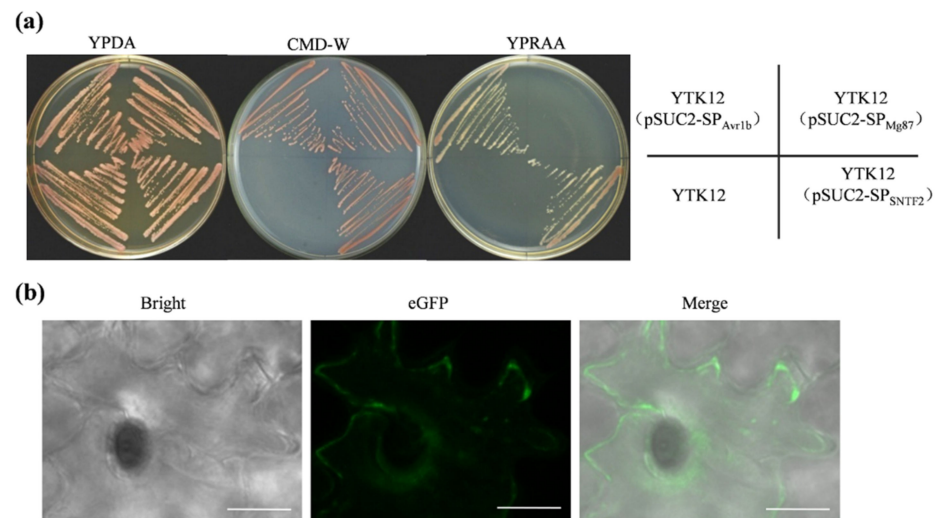


Figure 5. The secretory function validation of *Sntf2*. (a) The secretory function test of the predicted signal peptide (SP) of *Sntf2* was based on the yeast's secretory system. The YTK12 strains containing pSUC2-SP_{Avr1b} (SP_{Avr1b}: the SP sequence of *Avr1b* from *Phytophthora sojae*) were used as a positive control, and those containing pSUC2-SP_{Mg87} (SP_{Mg87}: the first 25 amino acids of *Mg87* protein from *Magnaporthe oryzae*) were used as negative controls. (b) *Sntf2*-eGFP fusion protein was translocated into plant cells during apple leaf infection. The leaves were inoculated with $\Delta sntf2-1/gpdAp:SNTF2:eGFP$ strain (*gpdAp*: the promoter of glyceraldehyde-3-phosphate dehydrogenase gene from *Aspergillus nidulans*). Bar: 10 μ m.

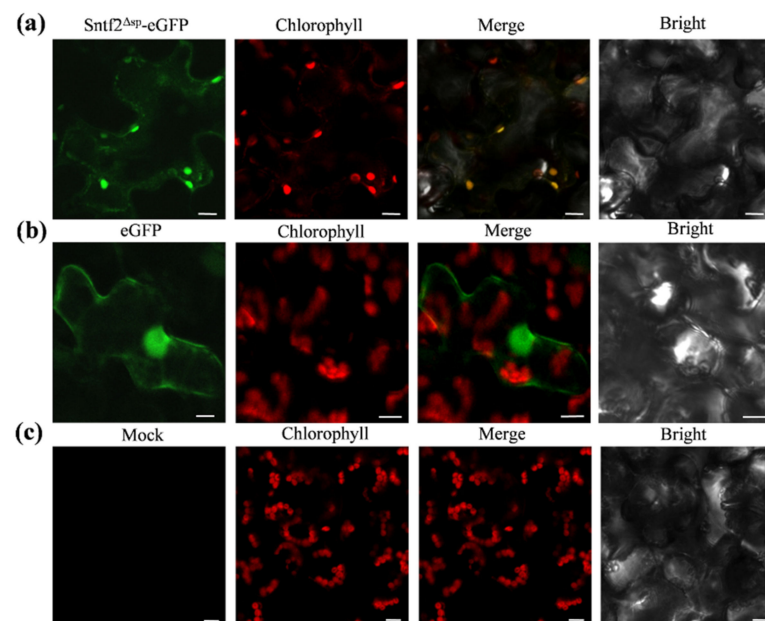


Figure 6. *Sntf2*^{ΔSP}-eGFP was localized to chloroplasts in *Nicotiana benthamiana*. (a) *Sntf2*^{ΔSP}-eGFP fluorescence signal overlapped with the chloroplasts autofluorescence signal. (b) The GFP protein was used as a control. (c) Mock. Bar: 10 μ m.

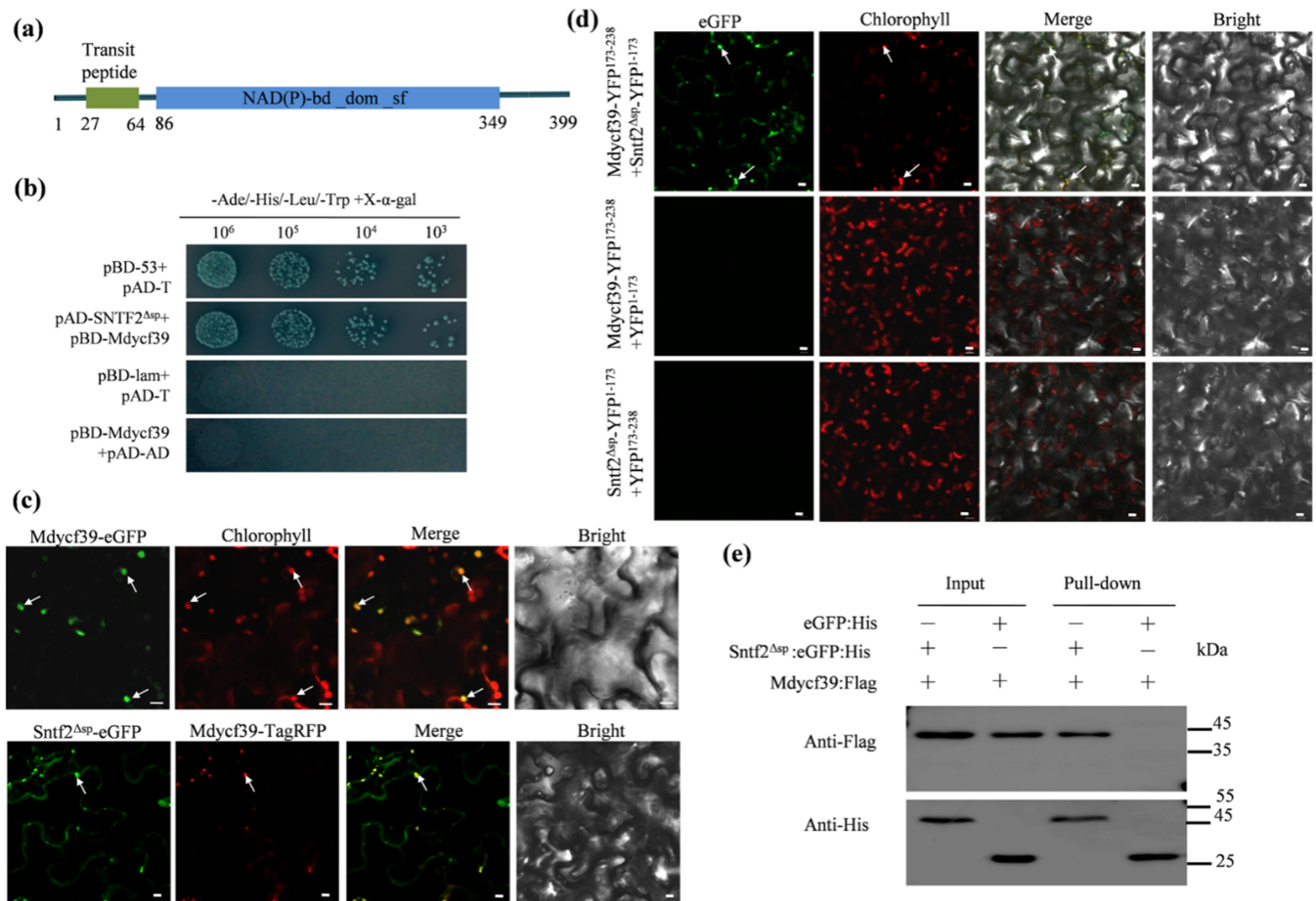


Figure 7. Sntf2 interacted with Mdyfc39 in chloroplasts. (a) Mdyfc39 was predicted to contain a chloroplast-targeting transit peptide and a NAD(P)-binding domain by the LOCALIZER program and InterPro 85.0. (b) Confirmation of the Sntf2–Mdyfc39 interaction using yeast two-hybrid assays. (c,d) Detection of the Sntf2–Mdyfc39 interaction using co-localization and bimolecular fluorescence complementation assays. The arrows refer to the chloroplasts. Bar: 10 μ m. (e) Confirmation of Sntf2–Mdyfc39 interaction using pull-down assays. Western blots for the analysis of Sntf2:eGFP:His and Mdyfc39:Flag purified proteins from *Escherichia coli* M15 and proteins from the His purification column using anti-His and anti-Flag antibodies. The Sntf2^{ΔSP}:eGFP:His and Mdyfc39:Flag bands were 46 and 45 kDa, respectively. The protein marker is labeled on the right.

The yeast two-hybrid assay revealed that Mdyfc39 interacted with Sntf2^{ΔSP} (lacking SP of Sntf2) (Figure 7b). We then transiently co-expressed the fuse proteins Sntf2^{ΔSP}-eGFP and Mdyfc39-TagRFP in *N. benthamiana*. The Mdyfc39-eGFP signal was detected in the chloroplasts, and the Mdyfc39-TagRFP signal was co-localized with the signal of Sntf2^{ΔSP}-eGFP (Figure 7c). The bimolecular fluorescence complementation (BiFC) assay revealed that the fluorescence signal of the interaction between Sntf2-YFP^{1–173} and Mdyfc39-YFP^{173–238} was present in chloroplasts (Figure 7d). The pull-down analysis also revealed that Sntf2^{ΔSP} interacted with Mdyfc39 (Figure 7e). These results showed that Sntf2 interacted with the PS II assembly factor Mdyfc39 in chloroplasts.

2.8. Mdyfc39 Overexpression Increases Susceptibility to *C. gloeosporioides* in Apple

To study the function of Mdyfc39 in plant infection by targeting Sntf2, we generated two Mdyfc39 overexpression transgenic lines (OE-yfc39-1 and OE-yfc39-2) and a Mdyfc39 transgenic silent line (Ri-yfc39) (Figure S7b,c). The OE-yfc39 lines showed no difference in plant growth compared with GL-3 (cv. Gala, a line) (Figure S7b), but they showed increased susceptibility to *C. gloeosporioides* compared with GL-3 (Figure S7d). However,

the disease severity of the OE-yfc39 lines was similar to that of GL-3 when inoculated with Δ sntf2-1 (Figure 8). The result indicated that Sntf2 may suppress apple defenses responses by targeting Mdyfc39. Unfortunately, the Ri-yfc39 line did not grow normally with pale-white leaves (Figure S7c), which was consistent with the phenotype of *hcf244* mutant in *Arabidopsis* [32], resulting in the abortion of the Ri-yfc39 line in the pathogenicity test. These results indicated that *Mdyfc39* played a vital role in plant resistance and development.

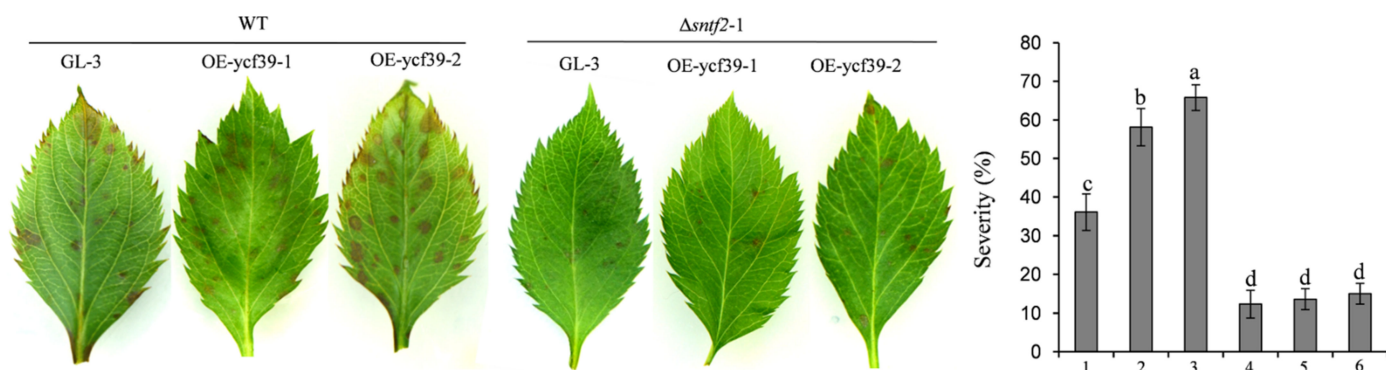


Figure 8. Analysis of the susceptibility of OE-yfc39 lines. The susceptibility was evaluated at three days after inoculation with WT and Δ sntf2-1 based on the disease index. 1–3: GL-3, OE-yfc39-1, and OE-yfc39-2 lines were inoculated with WT; 4–5: GL-3, OE-yfc39-1, and OE-yfc39-2 lines were inoculated with Δ sntf2-1. Three replicates were performed for each experiment, with six leaves for each replicate. Error bars represent standard deviations. Lowercase letters represent significant differences ($p < 0.01$).

3. Discussion

The effector plays a vital role in manipulating the host's immune responses and contributing to plant colonization by the pathogen [8,13,15]. In this study, we identified a novel effector Sntf2, which was required for the pathogenicity of *C. gloeosporioides*. *SNTF2* was highly expressed during the biotrophic infection phase. Effectors were induced to express and secreted to plant cells at different infection phases of *Colletotrichum* [33,34]. During the early biotrophic infection phase, effectors secreted to the plant cells interfered with immunity of the host, promoting the infection of the pathogen [34–36]. Indeed, in this study, we found that Sntf2 inhibited BAX-induced cell death, that the deletion of *SNTF2* induced callose deposition, and that H_2O_2 accumulation increased in infected leaves. These results indicated that Sntf2 played a role in suppressing plant defense and promoting biotrophic infection.

In this study, we found that Sntf2 interacted with Mdyfc39 (a PSII assembly factor of *Malus domestica*) in chloroplasts. Mdyfc39 is highly homologous to HCF244, a conserved PSII assembly factor in plants [32]. Mdyfc39 and HCF244 are homologous to Ycf39 of *Synechocystis* [37], which was demonstrated to participate in synthesis of the D1 (a subunit of PSII reaction centre) and assembly of the PSII in chloroplasts [32,37]. The synthesis of the D1 was necessary to maintain the structure and function of the PSII [38]. These suggested that Mdyfc39 may also be involved in the assembly of the PSII in chloroplasts of apples. In this study, the apple Mdyfc39-RNAi line did not grow normally on MS, consistent with the phenotype of *hcf244* mutant in *Arabidopsis* [32]. These results indicated that Mdyfc39 may affect the stability of PSII and play a role in plant growth and development.

Different suborganelles in the host often become targets of pathogens [23,39]. Many effectors target different components of the PSII in the host, which interferes with electron transport and inhibits ROS production, interfering with plant defense [6,28,40]. The effector RXLR31154 of *Plasmopara viticola* targets PsbP (a factor of the oxygen-evolving complex of PSII) to inhibit H_2O_2 production in a grapevine and enhance its susceptibility [6]. In our study, we found that the effector Sntf2 of *C. gloeosporioides* migrated into the host's

chloroplasts and interacted with Mdyf39. The transgenic overexpression lines of Mdyf39 in GL-3 showed an increased susceptibility to *C. gloeosporioides*. Our study indicated that Mdyf39 plays an important role in plant photosynthesis and defense responses. Mdyf39 may affect the stability of PSII and the production of H₂O₂ in chloroplasts. The defense response of plants is usually associated with ROS generation and callose depositions [41]. ROS has a direct anti-microbial role and is also a retrograde signaling molecule entering the nucleus to regulate the expression of defense-related genes, resulting in hypersensitive cell death [42–44]. In this study, the deletion of *SNTF2* increased the accumulation of H₂O₂ and the deposition of callose during infection. We speculated that Sntf2 perturbs the function of chloroplast by targeting Mdyf39, inhibiting the apple's defense response.

In conclusion, we identified a novel effector Sntf2 of *C. gloeosporioides*. Sntf2 is required for pathogenicity and plays a vital role in plant infection. The deletion of *SNTF2* triggers plant defense responses. Sntf2 secreted into the host cells was located in the chloroplast. Sntf2 interacted with Mdyf39 (a photosystem II assembly factor) in chloroplasts. We demonstrated that Sntf2 perturbs the function of chloroplasts by targeting Mdyf39, avoiding hypersensitive cell death, and supporting the colonization of *C. gloeosporioides* in apple leaves.

4. Materials and Methods

4.1. Strains and Plant Materials

The *C. gloeosporioides* strain W16 was used as the wild type (WT) strain [19]. The fungal strains were cultured on PDA plates at 26 °C as described previously [19]. For transformant selection, G-418 sulphate or hygromycin B was added to PDA in final concentrations of 500 µg/mL or 100 µg/mL, respectively [45]. The tissue-cultured 'GL-3' (cultivar 'Royal Gala') plants [46] and the transgenic plants were cultivated in MS medium [47] in a climate-controlled culture room at 25 ± 1 °C with a 16/8 h light/dark photoperiod as described by Dai et al. [46]. *N. benthamiana* seedlings were cultured in a greenhouse at 22–25 °C. The healthy leaves were obtained from 2-year-old seedlings of the 'Golden Delicious' variety of apples (*Malus domestica*) (Institute of Pomology of Chinese Academy of Agricultural Sciences, CAAS, Xingcheng, Liaoning Province, China).

4.2. *Agrobacterium tumefaciens* Infiltration Assays

The coding sequence of *SNTF2* (CGGC5_13909) was amplified and ligated into the potato virus X (PVX) vector pGR106 to generate pGR106-SNTF2. The primers used in this assay are listed in Table S2. The recombinant vector was transformed into *A. tumefaciens* GV3101. For transient expression in *N. benthamiana*, the transformant strains of GV3101 were infiltrated into the leaves. The experiment was performed as described by Shang et al. [15].

4.3. Vector Construction and Fungal Transformation

The gene deletion construction and transformation of *C. gloeosporioides* were carried out using the protocols described previously [45]. The gene complementation construction and the fungal transformation were performed as described previously [48]. The primers used in this assay are listed in Table S2. A detailed description is shown in Table S2. The putative gene knockout mutants were identified by PCR and Southern blot analysis. The complementation strains were confirmed based on PCR analysis.

4.4. Phenotype Assays

The hyphal growth rate and conidial production were assessed according to the method described by Zhou et al. [45]. The formation rates of appressorium and invasive pegs were observed and calculated as described by Shang et al. [15]. For plant inoculation, fresh conidial suspensions (1 × 10⁵ conidia/mL) were sprayed onto the apple leaves according to the method described by Zhou et al. [45]. The inoculated apple seedlings (2-year-old seedlings of the 'Golden Delicious' variety as shown in Section 4.1) were cultured at 28 °C and 75% humidity. For the pathogenicity test, the disease lesions were examined

3 days post-inoculation. The severity of the GLSA on each leaf was estimated using a diagrammatic scale [49].

4.5. RNA Extraction and qRT-PCR Analysis

The total RNA was extracted using an RNAprep Pure Plant Kit (TianGen Biotech, China Beijing). For the qRT-PCR analysis of *SNTF2*, the RNA samples of the infestation phase were obtained from 'Golden Delicious' leaves (2-year-old seedlings of the 'Golden Delicious' variety, inoculated as shown in Section 4.4) at 12, 24, 48, and 72 hpi. For the qRT-PCR analysis of *Mdyfc39*, the apple RNA samples were extracted from the transgenic overexpression lines of *Mdyfc39* and tissue-cultured 'GL-3' plants. The qRT-PCR was performed as described by Tan et al. [17]. The *M. domestica* ubiquitin extension (*MdUBQ*) was used as the endogenous reference gene [15].

4.6. Signal Peptide Activity Assay

The SP sequence of *SNTF2* was amplified and ligated into pSUC2 vector to generate pSUC2-SP_{SNTF2}. Recombinant vectors were transformed into the yeast strain YTK12, which lacks a secreted invertase [50]. All transformants were cultured on YPDA plates at 30 °C and cultured on CMD-W and YPRAA plates to assess if the invertase secreted. The enzyme activity of the invertase was evaluated based on the reduction of TTC to the insoluble red compound 1, 3, 5-triphenylformazan. The experiment was performed as described by Xu et al. [28].

4.7. Histochemical Assays

The H₂O₂ accumulation in plants was assessed using DAB staining as described by Chen et al. [51]. The samples were from 'GL-3' and transgenic leaves inoculated with the WT, $\Delta sntf2-1$, and $\Delta sntf2-1/SNTF2$ strains. DAB oxidation leads to brownish polymer formation and deposition at the site of ROS accumulation. The callose deposition was observed using aniline blue staining. The samples were decolorized by boiling in 96% ethanol for 5 min and then immersed in chloral hydrate overnight. The transparent leaf segments were stained with 0.05% aniline blue in 0.067 M K₂HPO₄ (pH 9.6) [28]. Then processed samples were preserved in 30% glycerol for microscopic analysis (Leica DM5000 B, Leica, Wetzlar, Germany). For every time point, either ten leaf discs were processed using DAB staining or aniline blue staining was obtained for ten leaf discs, and every experiment was performed three times. For every leaf disc, 100 appressoria were observed, and the percentage of ROS accumulation or callose deposition was calculated along with the means and standard deviations.

4.8. Yeast Two-Hybrid Assay

The coding sequences of *SNTF2* (without SP) were cloned into pGBKT7-BD as the bait, and the Matchmaker GAL4 system (OE Biotech, Shanghai, China) was used to screen a cDNA library constructed from RNA and isolated from different infection phases of the 'Golden Delicious' apple leaves. The screening was performed according to the manufacturer's instructions (OE Biotech, Shanghai, China). To confirm the interaction, the prey vector pAD-Sntf2^{ΔSP} and bait vector pBD-Mdyfc39 (constructed using *Mdyfc39* from 'Golden Delicious') were co-transformed into Y2Hgold yeast strains. The transformed yeast strains were grown on a medium (SD/-Leu/-Trp and SD/-Leu/-Trp/-His/-Ade) at 30 °C.

4.9. Transient Expression Analysis in *N. benthamiana*

For the subcellular localization assay, *SNTF2* (without SP) and *Mdyfc39* were cloned into pGR35s-eGFP or pGR35s-TagRFP and transformed into *A. tumefaciens* LBA4404 to express Sntf2^{ΔSP}-eGFP, Mdyfc39-eGFP, and Mdyfc39-TagRFP fusion proteins, respectively. The transient expression in *N. benthamiana* was performed as described by Xu et al. [28]. The *N. benthamiana* leaves were observed using a confocal microscope (Leica TCS SP8, Leica, Wetzlar, Germany) after 2 days of infiltration. For the BiFC assay, *SNTF2* and *Mdyfc39*

were ligated into the vectors pGR35s-YFP^{1–173} and pGR35s-YFP^{173–238}. The Mdyf39-YFP^{173–238} and Sntf2^{Δsp}-YFP^{1–173} fusion proteins were co-expressed by *A. tumefaciens* infiltration in *N. benthamiana*. The experiment was performed as described by Xu et al. [28]. GFP fluorescence was excited using a 488 nm laser, and emission was collected between 505 and 535 nm. YFP was excited using a 514 nm laser, and emission was collected between 530 and 560 nm. TagRFP was excited using a 555 nm laser, and emission was collected between 578 and 610 nm. For autofluorescent chloroplast detection, the excitation was 630 nm, and the collection range of emitted light was set at 650–681 nm [52].

4.10. Protein Extraction and Immunoblotting

For the pull-down assay, *SNTF2* and *Mdyf39* were cloned into pQE30-eGFP and pQE30-Flag and transformed into *Escherichia coli* M15 cells. Protein extraction was performed according to Dominguez-Martin et al. [53]. The induced proteins were observed using SDS-PAGE and Coomassie Brilliant Blue staining. The purified proteins were co-incubated on ice for 3 h and were purified using Ni-NTA beads (CW0894S, CWBIO, Beijing, China). For immune detection, the purified proteins were transferred to a polyvinylidene fluoride membrane. The corresponding mouse anti-His or mouse anti-Flag (1:1000; cat. no. HT201, TransGenBiotech, Beijing, China) antibody was used as the primary antibody, respectively. The HRP-labelled goat anti-mouse IgG (1:2000; cat. no. A0216, Beyotime, Shanghai, China) was used as the secondary antibody. The membrane was treated with a BeyoECL Star kit (Beyotime, Shanghai, China) for 2 min. Images were acquired using a BIO-RAD ChemiDoc™ Imaging System.

4.11. Generation of Transgenic ‘GL-3’ Plants with *Mdyf39* Overexpression or RNA-Interference

Mdyf39 was amplified and inserted into the pRNAi and pRPHA vectors to generate the RNAi transgenic silenced line Ri-yf39 as well as the transgenic overexpression lines OE-yf39. The *Agrobacterium*-mediated transformation of ‘GL-3’ was performed as described by Dai et al. [46]. *A. tumefaciens* LBA4404 was used for the stable transformations.

Supplementary Materials: The following are available online at <https://www.mdpi.com/article/10.3390/ijms23126379/s1>.

Author Contributions: Conceptualization, Z.Z.; methodology, M.W., J.X., X.Z. and Z.Z.; software, M.W., J.X. and Z.J.; validation, M.W., Z.J. and H.Y.; formal analysis, M.W. and Z.J.; investigation, M.W., H.Y. and X.Z.; resources, Z.Z. and Z.J.; data curation, M.W.; writing—original draft preparation, M.W.; writing—review and editing, Z.Z.; visualization, M.W.; supervision, Z.Z. and Z.J.; project administration, Z.Z.; funding acquisition, Z.Z. All authors have read and agreed to the published version of the manuscript.

Funding: This work was supported by The Agricultural Science and Technology Innovation Program of the Chinese Academy of Agricultural Sciences (CAAS-ASTIP-2016-RIP), China Agriculture Research System of MOF and MARA (CARS-27), and Special Funds for Basic Scientific Research Operation of Central-level Public Welfare Scientific Research Institutes (1610182019030).

Institutional Review Board Statement: Not applicable.

Informed Consent Statement: Not applicable.

Data Availability Statement: The data presented in this study are available in the article.

Acknowledgments: The authors would like to thank Zhang Zhi-hong, (Shenyang Agricultural University), for providing tissue-cultured ‘GL-3’ (cultivar ‘Royal Gala’) plants. Thank you, Dou Dao-long, (College of Plant Protection, Nanjing Agricultural University), for the pGR106 vector.

Conflicts of Interest: The authors declare no conflict of interest.

References

1. Chisholm, S.T.; Coaker, G.; Day, B.; Staskawicz, B.J. Host-microbe interactions: Shaping the evolution of the plant immune response. *Cell* **2006**, *124*, 803–814. [\[CrossRef\]](#)
2. Jones, J.D.G.; Dangl, J.L. The plant immune system. *Nature* **2006**, *444*, 323–329. [\[CrossRef\]](#) [\[PubMed\]](#)
3. Marco, Z.; Massimiliano, C.; Antonio, K.M.; Antonielle, M.; Silvia, M.; Irma, M.; Sylvie, J.; de Ortiz, G.M.; Christian, H.; Mathilde, F.; et al. LPMO-oxidized cellulose oligosaccharides evoke immunity in *Arabidopsis* conferring resistance towards necrotrophic fungus *B. cinerea*. *Commun. Biol.* **2021**, *4*, 4224.
4. Kubicek, C.P.; Starr, T.L.; Glass, N.L. Plant Cell Wall-Degrading Enzymes and Their Secretion in Plant-Pathogenic Fungi. *Annu. Rev. Phytopathol.* **2014**, *52*, 427–451. [\[CrossRef\]](#)
5. Dou, D.; Zhou, J.M. Phytopathogen effectors subverting host immunity: Different foes, similar battleground. *Cell Host Microbe* **2012**, *12*, 484–495. [\[CrossRef\]](#)
6. Liu, R.; Chen, T.; Yin, X.; Xiang, G.; Peng, J.; Fu, Q.; Xu, Y. A *Plasmopara viticola* RxLR effector targets a chloroplast protein PsbP to inhibit ROS production in grapevine. *Plant J.* **2021**, *106*, 1557–1570. [\[CrossRef\]](#)
7. Perfect, S.E.; Hughes, H.B.; O’Connell, R.J.; Green, J.R. *Colletotrichum*: A Model Genus for Studies on Pathology and Fungal-Plant Interactions. *Fungal Genet. Biol.* **1999**, *27*, 186–198. [\[CrossRef\]](#)
8. Bhadauria, V.; Banniza, S.; Vandenberg, A.; Selvaraj, G.; Wei, Y. Overexpression of a novel biotrophy-specific *Colletotrichum truncatum* effector, CtnUDIX, in hemibiotrophic fungal phytopathogens causes incompatibility with their host plants. *Eukaryot. Cell* **2013**, *12*, 2–11. [\[CrossRef\]](#) [\[PubMed\]](#)
9. Yoshino, K.; Irieda, H.; Sugimoto, F.; Yoshioka, H.; Okuno, T.; Takano, Y. Cell death of *Nicotiana benthamiana* is induced by secreted protein NIS1 of *Colletotrichum orbiculare* and is suppressed by a homologue of CgDN3. *Mol. Plant-Microbe Interact. MPMI* **2012**, *25*, 625. [\[CrossRef\]](#)
10. Takahara, H.; Hacquard, S.; Kombrink, A.; Hughes, H.B.; Halder, V.; Robin, G.P.; Hiruma, K.; Neumann, U.; Shinya, T.; Kombrink, E. *Colletotrichum higginsianum* extracellular LysM proteins play dual roles in appressorial function and suppression of chitin-triggered plant immunity. *New Phytol.* **2016**, *211*, 1323–1337. [\[CrossRef\]](#)
11. Takahara, H.; Yamaguchi, S.; Omura, N.; Nakajima, S.; Otoku, K.; Tanaka, S.; Ogura, K.; Kleemann, J.; O’Connell, R. The *Colletotrichum higginsianum* secreted effector protein ChEC91 induces plant cell death. *J. Gen. Plant Pathol.* **2021**, *87*, 344–353. [\[CrossRef\]](#)
12. Ayako, T.; Mari, N.; Pamela, G.; Naoyoshi, K.; Ryoko, H.; Naoki, K.; Shunji, T.; Yoshitaka, T.; Yoshihiro, N.; Ken, S. The conserved *Colletotrichum spp.* effector candidate CEC3 induces nuclear expansion and cell death in plants. *Front. Microbiol.* **2021**, *12*, 682155.
13. Kleemann, J.; Rinconrivera, L.J.; Takahara, H.; Neumann, U.; van Themaat, E.V.L.; Hc, V.D.D.; Hacquard, S.; Stüber, K.; Will, I.; Schmalenbach, W. Correction: Sequential delivery of host-induced virulence effectors by appressoria and intracellular hyphae of the phytopathogen *Colletotrichum higginsianum*. *PLoS Pathog.* **2012**, *8*, e1002643. [\[CrossRef\]](#)
14. Irieda, H.; Maeda, H.; Akiyama, K.; Hagiwara, A.; Saitoh, H.; Uemura, A.; Terauchi, R.; Takano, Y. *Colletotrichum orbiculare* secretes virulence effectors to a biotrophic interface at the primary hyphal neck via exocytosis coupled with SEC22-mediated traffic. *Plant Cell* **2014**, *26*, 2265–2281. [\[CrossRef\]](#)
15. Shang, S.; Wang, B.; Zhang, S.; Liu, G.; Liang, X.; Zhang, R.; Gleason, M.L.; Sun, G. A novel effector CfEC92 of *Colletotrichum fructicola* contributes to glomerella leaf spot virulence by suppressing plant defences at the early infection phase. *Mol. Plant Pathol.* **2020**, *21*, 936–950. [\[CrossRef\]](#) [\[PubMed\]](#)
16. Crouch, J.A.; O’Connell, R.; Gan, P.; Buiate, E.; Torres, M.F.; Beirn, L.; Shirasu, K.; Vaillancourt, L. The Genomics of *Colletotrichum*. In *Genomics of Plant-Associated Fungi: Monocot Pathogens*; Springer: Berlin/Heidelberg, Germany, 2014.
17. Tan, Q.; Zhao, X.; He, H.; Zhang, J.; Yi, T. Carbamoyl phosphate synthetase subunit Cpa1 interacting with Dut1, controls development, arginine biosynthesis, and pathogenicity of *Colletotrichum gloeosporioides*. *Fungal Biol.* **2020**, *125*, 184–190. [\[CrossRef\]](#) [\[PubMed\]](#)
18. Yakoby, N.; Beno-Moualem, D.; Keen, N.T.; Dinoor, A.; Pines, O.; Prusky, D. *Colletotrichum gloeosporioides* pelB Is an Important Virulence Factor in Avocado Fruit-Fungus Interaction. *Mol Plant Microbe Interact* **2001**, *14*, 988–995. [\[CrossRef\]](#)
19. Wu, J.; Ji, Z.; Wang, N.; Chi, F.; Xu, C.; Zhou, Z.; Zhang, J. Identification of conidiogenesis-associated genes in *Colletotrichum gloeosporioides* by agrobacterium tumefaciens-mediated transformation. *Curr. Microbiol.* **2016**, *73*, 802–810. [\[CrossRef\]](#)
20. Gonzalez, E.; Sutton, T.B. First report of Glomerella leaf spot (*Glomerella cingulata*) of apple in the United States. *Plant Dis.* **1999**, *83*, 1074. [\[CrossRef\]](#)
21. Wang, C.X.; Zhang, Z.F.; Li, B.H.; Wang, H.Y.; Dong, X.L. First report of Glomerella Leaf spot of apple caused by *Glomerella cingulata* in China. *Plant Dis.* **2012**, *96*, 912. [\[CrossRef\]](#)
22. González, E.; Sutton, T.B.; Correll, J.C. Clarification of the Etiology of Glomerella Leaf Spot and Bitter Rot of Apple Caused by *Colletotrichum spp.* Based on Morphology and Genetic, Molecular, and Pathogenicity Tests. *Phytopathology* **2006**, *96*, 982. [\[CrossRef\]](#) [\[PubMed\]](#)
23. De Torres Zabala, M.; Littlejohn, G.; Jayaraman, S.; Studholme, D.; Bailey, T.; Lawson, T.; Tillich, M.; Licht, D.; Bölter, B.; Delfino, L.; et al. Chloroplasts play a central role in plant defence and are targeted by pathogen effectors. *Nat. Plants* **2015**, *1*, 15074. [\[CrossRef\]](#)
24. Chan, K.X.; Phua, S.Y.; Crisp, P.; McQuinn, R.; Pogson, B.J. Learning the languages of the chloroplast: Retrograde signaling and beyond. *Annu. Rev. Plant Biol.* **2016**, *67*, 25–53. [\[CrossRef\]](#)

25. Medina-Puche, L.; Tan, H.; Dogra, V.; Wu, M.; Lozano-Duran, R. A defense pathway linking plasma membrane and chloroplasts and co-opted by pathogens. *Cell* **2020**, *182*, 1109–1124. [[CrossRef](#)]
26. Serrano, I.; Audran, C.; Rivas, S. Chloroplasts at work during plant innate immunity. *J. Exp. Bot.* **2016**, *67*, 3845–3854. [[CrossRef](#)] [[PubMed](#)]
27. Nomura, H.; Komori, T.; Uemura, S.; Kanda, Y.; Shimotani, K.; Nakai, K.; Furuichi, T.; Takebayashi, K.; Sugimoto, T.; Sano, S.; et al. Chloroplast-mediated activation of plant immune signalling in *Arabidopsis*. *Nat. Commun.* **2012**, *3*, 926. [[CrossRef](#)]
28. Xu, Q.; Tang, C.; Wang, X.; Sun, S.; Zhao, J.; Kang, Z.; Wang, X. An effector protein of the wheat stripe rust fungus targets chloroplasts and suppresses chloroplast function. *Nat. Commun.* **2019**, *10*, 5571. [[CrossRef](#)]
29. Rosas-Diaz, T.; Zhang, D.; Fan, P.; Wang, L.; Ding, X.; Jiang, Y.; Jimenez-Gon-gora, T.; Medina-Puche, L.; Zhao, X.; Feng, Z. A virus-targeted plant receptor-like kinase promotes cell-to-cell spread of RNAi. *Proc. Natl. Acad. Sci. USA* **2018**, *115*, 1388–1393. [[CrossRef](#)] [[PubMed](#)]
30. Lacomme, C.; Santa, C.S. Bax-induced cell death in tobacco is similar to the hypersensitive response. *Proc. Natl. Acad. Sci. USA* **1999**, *96*, 7956–7961. [[CrossRef](#)]
31. Weixiao, Y.; Yufu, W.; Tao, C.; Yang, L.; Chaoxi, L. Functional Evaluation of the Signal Peptides of Secreted Proteins. *Bio-Protoc.* **2018**, *8*, e2839.
32. Link, S.; Engelmann, K.; Meierhoff, K.; Westhoff, P. The atypical short-chain dehydrogenases HCF173 and HCF244 are jointly involved in translational initiation of the psbA mRNA of *Arabidopsis*. *Plant Physiol.* **2012**, *160*, 2202–2218. [[CrossRef](#)]
33. De Queiroz, C.B.; Correia, H.L.N.; Santana, M.F. The repertoire of effector candidates in *Colletotrichum lindemuthianum* reveals important information about *Colletotrichum* genus lifestyle. *Appl. Microbiol. Biotechnol.* **2019**, *103*, 2295–2309. [[CrossRef](#)]
34. Gan, P.; Ikeda, K.; Irieda, H.; Narusaka, M.; O’Connell, R.J.; Narusaka, Y.; Takano, Y.; Kubo, Y.; Shirasu, K. Comparative genomic and transcriptomic analyses reveal the hemibiotrophic stage shift of *Colletotrichum* fungi. *New Phytol.* **2013**, *197*, 1236–1249. [[CrossRef](#)] [[PubMed](#)]
35. Liang, X.; Shang, S.; Dong, Q.; Wang, B.; Zhang, R.; Mark, L.G.; Sun, G. Transcriptomic analysis reveals candidate genes regulating development and host interactions of *Colletotrichum fructicola*. *Bmc. Genom.* **2018**, *19*, 557. [[CrossRef](#)] [[PubMed](#)]
36. O’Connell, R.J.; Thon, M.R.; Hacquard, S.; Amyotte, S.G.; Kleemann, J.; Torres, M.F.; Damm, U.; Buiate, E.A.; Epstein, L.; Alkan, N. Lifestyle transitions in plant pathogenic *Colletotrichum* fungi deciphered by genome and transcriptome analyses. *Nat. Genet.* **2012**, *44*, 1060–1065. [[CrossRef](#)]
37. Knoppova, J.; Sobotka, R.; Tichy, M.; Yu, J.; Konik, P.; Halada, P.; Nixon, P.J.; Komenda, J. Discovery of a chlorophyll binding protein complex involved in the early steps of photosystem II assembly in *Synechocystis*. *Plant Cell* **2014**, *26*, 1200–1212. [[CrossRef](#)]
38. Andersson, B.; Aro, E.M. Photodamage and D1 Protein Turnover in Photosystem II. *Regul. Photosynth.* **2001**, *11*, 377–393.
39. Robin, G.P.; Kleemann, J.; Neumann, U.; Cabre, L.; Dallery, J.F.; Lapalu, N.; O’Connell, R.J. Subcellular Localization Screening of *Colletotrichum higginsianum* Effector Candidates Identifies Fungal Proteins Targeted to Plant Peroxisomes, Golgi Bodies, and Microtubules. *Front. Plant Sci.* **2018**, *9*, 562. [[CrossRef](#)] [[PubMed](#)]
40. Herva, J.J.R.; Melendi, P.G.; Lanza, R.C.; Lamas, M.A.; Alvarez, I.R.; Li, Z.; Torrejón, G.L.; Díaz, I.; de Pozo, J.C.; Chakravarthy, S.; et al. A bacterial cysteine protease effector protein interferes with photosynthesis to suppress plant innate immune responses. *Cell. Microbiol.* **2012**, *14*, 669–681. [[CrossRef](#)]
41. Couto, D.; Zipfel, C. Regulation of pattern recognition receptor signalling in plants. *Nat. Rev. Immunol.* **2016**, *16*, 537–552. [[CrossRef](#)]
42. Torres, M.A. ROS in biotic interactions. *Physiol. Plant.* **2010**, *138*, 414–429. [[CrossRef](#)] [[PubMed](#)]
43. Galvez-Valdivieso, G.; Mullineaux, P.M. The role of reactive oxygen species in signalling from chloroplasts to the nucleus. *Physiol. Plant* **2010**, *138*, 430–439. [[CrossRef](#)]
44. Quan, L.J.; Zhang, B.; Shi, W.-W.; Li, H.-Y. Hydrogen Peroxide in Plants: a Versatile Molecule of the Reactive Oxygen Species Network. *J. Integr. Plant Biol.* **2008**, *50*, 2–18. [[CrossRef](#)]
45. Zhou, Z.; Wu, J.; Wang, M.; Zhang, J. ABC protein CgABC2 is required for asexual and sexual development, appressorial formation and plant infection in *Colletotrichum gloeosporioides*. *Microb. Pathog.* **2017**, *110*, 85–92. [[CrossRef](#)]
46. Dai, H.; Li, W.; Han, G.; Yi, Y.; Zhang, Z. Development of a seedling clone with high regeneration capacity and susceptibility to *Agrobacterium* in apple. *Sci. Hortic.* **2013**, *164*, 202–208. [[CrossRef](#)]
47. Srinivasan, C.; Liu, Z.; Scorza, R. Ectopic expression of class 1 KNOX genes induce adventitious shoot regeneration and alter growth and development of tobacco (*Nicotiana tabacum* L.) and European plum (*Prunus domestica* L.). *Plant Cell Rep.* **2011**, *30*, 655–664. [[CrossRef](#)]
48. Zhao, X.; Tang, B.; Xu, J.; Wang, N.; Zhou, Z.; Zhang, J. A SET domain-containing protein involved in cell wall integrity signaling and peroxisome biogenesis is essential for appressorium formation and pathogenicity of *Colletotrichum gloeosporioides*. *Fungal Genet. Biol.* **2020**, *145*, 103474. [[CrossRef](#)]
49. Bogo, A.; Casa, T.R.; Rufato, L.; Goncalves, J.M. The effect of hail protection nets on *Glomerella* leaf spot in ‘Royal Gala’ apple. *Crop Prot.* **2012**, *31*, 40–44. [[CrossRef](#)]
50. Gietz, R.D.; Schiestl, R.H.; Willems, A.R.; Woods, R.A. Studies on the transformation of intact yeast cells by the LiAc/SS-DNA/PEG procedure. *Yeast* **1995**, *11*, 355–360. [[CrossRef](#)]
51. Chen, M.; Zeng, H.; Qiu, D.; Guo, L.; Yang, X.; Shi, H.; Zhou, T.; Zhao, J. Purification and characterization of a novel hypersensitive response-inducing elicitor from *Magnaporthe oryzae* that triggers defense response in rice. *PLoS ONE* **2012**, *7*, e37654. [[CrossRef](#)]

52. Feng, Q.; Wang, W.; Li, H.; Pan, X. Autofluorescence of chloroplasts measured by a laser scanning confocal microscope. *J. Tsinghua Univ. (Sci. Technol.)* **2017**, *57*, 651–654.
53. Dominguez-Martin, M.A.; Polívka, T.; Sutter, M.; Ferlez, B.; Lechno-Yossef, S.; Montgomery, B.L.; Kerfeld, C.A. Structural and spectroscopic characterization of HCP2. *Biochim. Biophys. Acta Bioenerg.* **2019**, *1860*, 414–424. [[CrossRef](#)]